Rovibrational population transfer in the ground state controlled by two coherent laser pulses

Rong Wang,[1] Ying-Yu Niu,[1,*] Ming-Hui Qiu,[1] and Yong-Chang Han[2]
[1]*School of Science, Dalian Jiaotong University, Dalian 116028, China*
[2]*Department of Physics, Dalian University of Technology, Dalian 116024, China*
(Received 26 October 2013; revised manuscript received 19 November 2014; published 5 January 2015)

A time-dependent quantum wave-packet method is employed to investigate the rovibrational dynamics of population transfer in the ground electronic state controlled by two-color ($\omega + 2\omega$) pulses analogous to coherently control the processes of ionization and dissociation. The population can be transferred to three target states, $|4,1\rangle$, $|0,1\rangle$, and $|4,0\rangle$, at the same time through the ladder Λ and multiphoton transitions. With the variation of the relative phase between ω and 2ω pulses, the population distributions show oscillation behavior with a period of π. The population variation with relative phase depends on the size of the electric field asymmetry. The probabilities transferred to different target states can be controlled by varying the pulse amplitudes.

DOI: 10.1103/PhysRevA.91.013401 PACS number(s): 33.80.Be, 37.10.Vz, 42.50.Hz, 82.20.Bc

I. INTRODUCTION

The interaction of molecules with the laser field has long been an important subject in photophysics and photochemistry. With properly designed parameters of the laser pulses, such as the duration, carrier frequency, shape, peak intensity, and phase of pulses, the population of molecules can be completely localized at well-defined quantum states on picosecond or femtosecond time scales [1–4]. Several approaches are theoretically proposed to control population transfer by chirped laser pulses, adiabatic passage, multipath interference, and optimal control theory [5–9]. The laser field to control selective excitation is often composed of one or more pulses. Andrianov and Paramonov employed four partly overlapping 1-ps laser pulses to prepare a moderately high rovibrational state $|11,4\rangle$ in the ground electronic state [10].

The two-laser-pulse scheme is an important way to control population transfer. In this scheme, two partly overlapping laser pulses are employed, and population can be transferred from a initial state to a target state via one or more intermediate states. According to the excitation pathway, the process of population transfer can be divided into Λ and ladder systems. These two systems have been investigated theoretically as well as experimentally [11–15]. We have previously studied the population transfer process through a stimulated Raman adiabatic passage (STIRAP) scheme controlled by two incoherent pulses [16]. On the picosecond or subpicosecond time scales, the initial phases of the laser pulses usually have a weak effect on the final population and can be neglected [10].

The two laser pulses with frequency ω and its second harmonic 2ω have been used to ionize and dissociate molecules [17–20]. The relative phase between two harmonic pulses is sufficient to coherently control the processes of ionization and dissociation, such as the angular distributions of the photoelectron and the photofragment branching ratio of dissociated molecules [21,22]. Sheehy *et al.* reported that the photodissociation of the HD^+ molecule ion can be coherently controlled by the relative phase between a two-color optical field [23].

In this article, we employ a time-dependent quantum wave-packet method to investigate rovibrational population transfer in a ground electronic state of HF molecules controlled by two-color ($\omega + 2\omega$) laser pulses. In our model, the initial state is $|0,0\rangle$, and the target states are $|4,1\rangle$ and $|0,1\rangle$. The transitions $|0,0\rangle \rightarrow |4,1\rangle$ and $|0,0\rangle \rightarrow |0,1\rangle$ are achieved through the ladder and Λ systems. The processes of these two transitions include six intermediate states and two excitation pathways, respectively. The relations between the final population and the relative phase are discussed, and the effects of the pulse parameters and electric field shape on the population distributions are examined in detail.

II. THEORETICAL METHOD

In our theoretical model, only the ground electronic state of HF molecule is taken into account. The total electric field, a superposition of two infrared laser pulses, is expressed as

$$\varepsilon(t) = E_1 f_1(t)\cos[\omega(t - t_{01})] + E_2 f_2(t)\cos[2\omega(t - t_{02}) + \phi], \tag{1}$$

where E_1 and E_2 are the electric field amplitudes, ϕ is the relative phase, and t_{01} and t_{02} are the start times of the two pulses. The envelopes $f_i(t)$ of the pulses are given by

$$f_i(t) = \sin^2\left[\frac{\pi(t - t_{0i})}{\tau_i}\right], \quad i = 1,2, \tag{2}$$

where τ_i denotes the duration of the ith pulse. In the present work, we assume the initial state to be $|\nu = 0, j = 0\rangle$ with magnetic quantum number $M = 0$. In the linearly polarized laser field, only the $\Delta M = 0$ transition is considered, and the interaction between the molecule and laser field can be written as

$$\hat{W}(t) = -\mu(R)\cos(\theta)\varepsilon(t), \tag{3}$$

where θ is the angle between the molecular axis and the laser electric field direction. The function of the molecular permanent dipole moment $\mu(R)$ is obtained from Ref. [10]. In the Born-Oppenheimer approximation, the quantum dynamics of the molecule can be described by the time-dependent

*niuyy@djtu.edu.cn

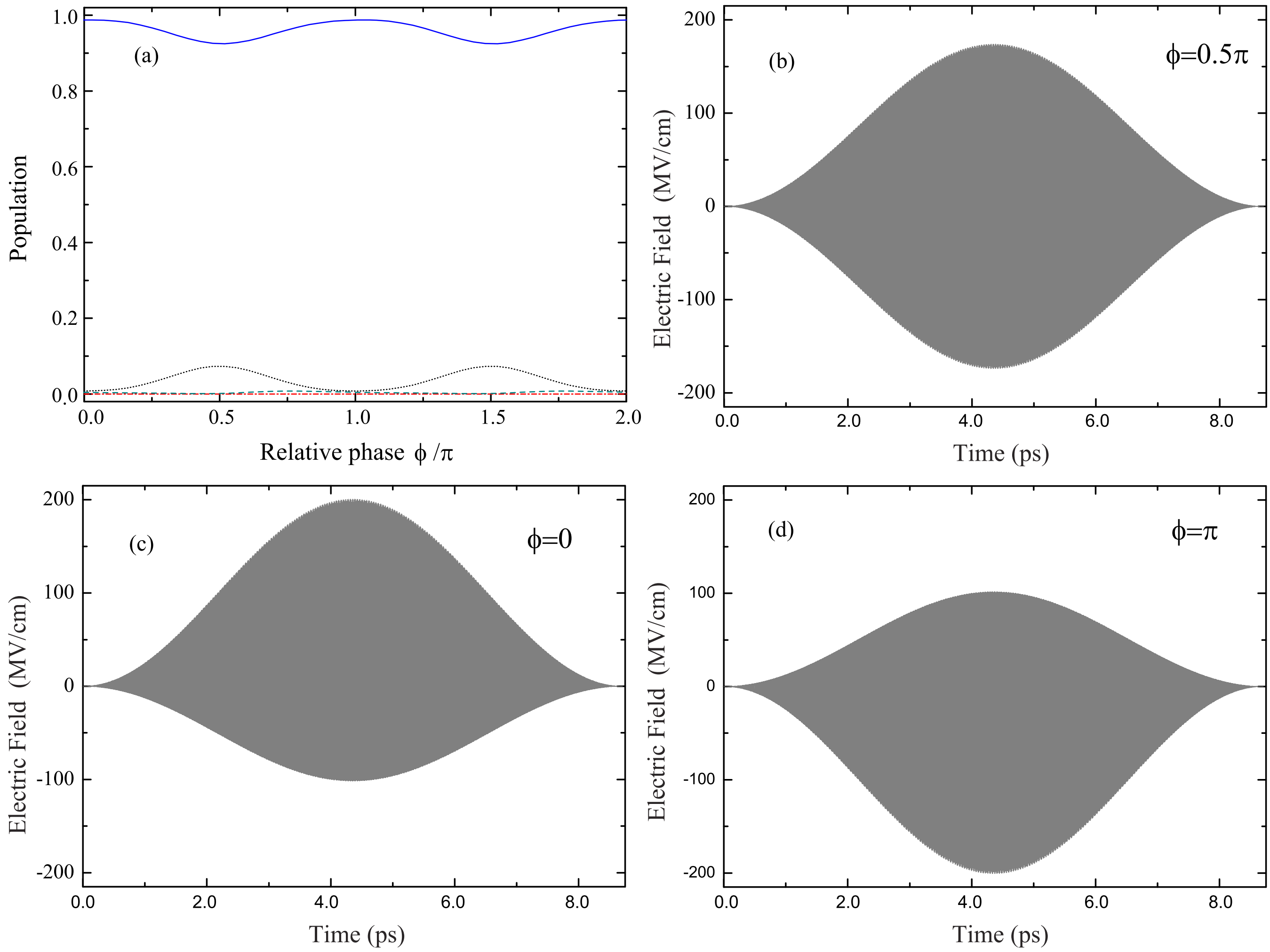

FIG. 1. (Color online) (a) The population distributions versus the relative phase ϕ. The solid, dot, dashed, and dot-dashed curves represent the states $|4,1\rangle$, $|0,0\rangle$, $|4,0\rangle$, and $|0,1\rangle$, respectively. (b) The total electric field with $\phi = 0.5\pi$. (c) The total electric field with $\phi = 0$. (d) The total electric field with $\phi = \pi$. The laser parameters are chosen to be $E_1 = 141.90$ MV/cm, $E_2 = 58.88$ MV/cm, $\tau_1 = \tau_2 = 8.708$ ps, $t_{01} = t_{02} = 0$ ps.

Schrödinger equation

$$i\hbar\frac{\partial}{\partial t}\Psi(t) = [\hat{T}_R + \hat{T}_\theta + \hat{U}(R) + \hat{W}(t)]\Psi(t), \tag{4}$$

the potential energy $\hat{U}(R)$ is described by the Morse potential function, and the parameters of the function are adapted from Ref. [10]. The kinetic-energy terms are given by

$$\hat{T}_R = -\frac{\hbar^2}{2m}\frac{\partial^2}{\partial R^2} \tag{5}$$

and

$$\hat{T}_\theta = -\frac{\hbar^2}{2mR^2}\frac{1}{\sin\theta}\frac{\partial}{\partial\theta}\left(\sin\theta\frac{\partial}{\partial\theta}\right), \tag{6}$$

where R is the internuclear separation, and m is the reduced mass of HF molecule.

The rovibrational eigenfunction $|\nu, j\rangle$ is a direct product of the function $\phi_{\nu,j}$ and the Legendre polynomial $P_j(\cos\theta)$. $\phi_{\nu,j}$ is the $j-$dependent radial vibrational function, which can be obtained by using the Fourier grid Hamiltonian method [24]. Here we choose the eigenfunction $|0,0\rangle$ as the initial function.

The time propagation of the Schrödinger equation (4) is accomplished by using the split operator method [10,25]. The time-dependent rovibrational population $P_{\nu,j}$ can be obtained by the projection of wave function on rovibrational eigenstates $|\nu, j\rangle$,

$$P_{\nu,j} = |\langle \nu, j|\Psi(t)\rangle|^2. \tag{7}$$

III. RESULTS AND DISCUSSION

As the fundamental frequency ω is chosen as 3704.36 cm^{-1}, which satisfies the multiphoton resonance condition between the states $|0,0\rangle$ and $|4,0\rangle$, the population can be transferred to the state $|4,0\rangle$ through the four-photon transition

$$|0,0\rangle \xrightarrow{\omega} |1,1\rangle \xrightarrow{\omega} \left\{\begin{matrix}|2,0\rangle\\|2,2\rangle\end{matrix}\right\} \xrightarrow{\omega} |3,1\rangle \xrightarrow{\omega} |4,0\rangle \tag{8}$$

and two-photon transition [26]

$$|0,0\rangle \xrightarrow{2\omega} |2,1\rangle \xrightarrow{2\omega} |4,0\rangle. \tag{9}$$

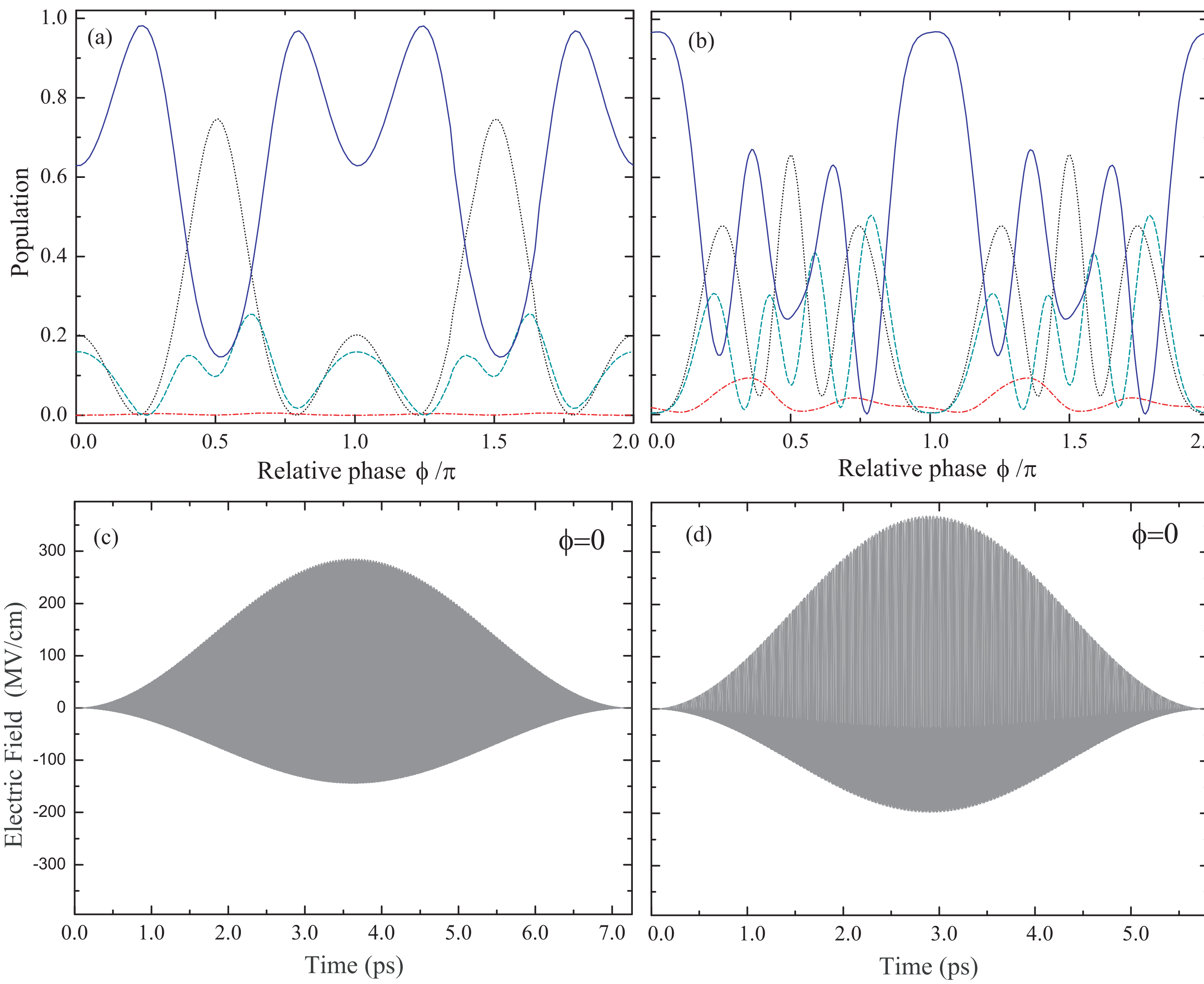

FIG. 2. (Color online) (a) and (b) The population distributions versus the relative phase ϕ. The solid, dot, dashed, and dot-dashed curves in each graph represent the states $|4,1\rangle$, $|0,0\rangle$, $|4,0\rangle$, and $|0,1\rangle$, respectively. (c) The total electric field with $\phi = 0$. The laser parameters are chosen to be $E_1 = 177.92$ MV/cm, $E_2 = 108.19$ MV/cm, $\tau_1 = \tau_2 = 7.257$ ps, $t_{01} = t_{02} = 0$ ps. (d) The total electric field with $\phi = 0$. The laser parameters are chosen to be $E_1 = 202.06$ MV/cm, $E_2 = 167.89$ MV/cm, $\tau_1 = \tau_2 = 5.805$ ps, $t_{01} = t_{02} = 0$ ps.

Here we choose the fundamental frequency as 3708.68 cm^{-1}. With this frequency, the transition probability for the multiphoton transitions is reduced, and the population can be transferred to the other target states through ladder and Λ transitions.

We first consider a ladder system in which the population in the initial state $|0,0\rangle$ is transferred to the target state $|4,1\rangle$. In most cases, the ladder transition is induced by a two incoherent pulse system [11,12]. The relative phase of two incoherent pulses has a weak effect on the final population, and the population transfer is achieved through only one excitation pathway. In our model, the two pulses with ω and 2ω can drive population transfer through two transitions: the (2+1) pathway,

$$|0,0\rangle \xrightarrow{\omega} |1,1\rangle \xrightarrow{\omega} \left\{ \begin{matrix} |2,0\rangle \\ |2,2\rangle \end{matrix} \right\} \xrightarrow{2\omega} |4,1\rangle, \tag{10}$$

and the (1+2) pathway,

$$|0,0\rangle \xrightarrow{2\omega} |2,1\rangle \xrightarrow{\omega} \left\{ \begin{matrix} |3,0\rangle \\ |3,2\rangle \end{matrix} \right\} \xrightarrow{\omega} |4,1\rangle. \tag{11}$$

Figure 1 shows the population distributions as a function of the relative phase ϕ. The two pulse durations are 8.708 ps, and the amplitudes of the two pulses are optimized to produce a nearly 100% population in the state $|4,1\rangle$. It can been seen from Fig. 1(a) that the population mainly stays in the initial state $|0,0\rangle$ and target state $|4,1\rangle$. The population of the target state reaches the maximum value (98.8%) at $\phi = 0$ and π. When the relative phase is chosen as 0.5π or 1.5π, $P_{4,1}$ is the minimum value (92.5%), and about 7.3% of population stays in the initial state $|0,0\rangle$. For two harmonic pulses, the symmetry of the total electric field is a function of the relative phase [23]. In Fig. 1(b) the case $\phi = \pi/2$ corresponds to a symmetric field. The largest asymmetries are at $\phi = 0$, with the smaller amplitude in the negative direction, and at $\phi = \pi$, with the smaller amplitude

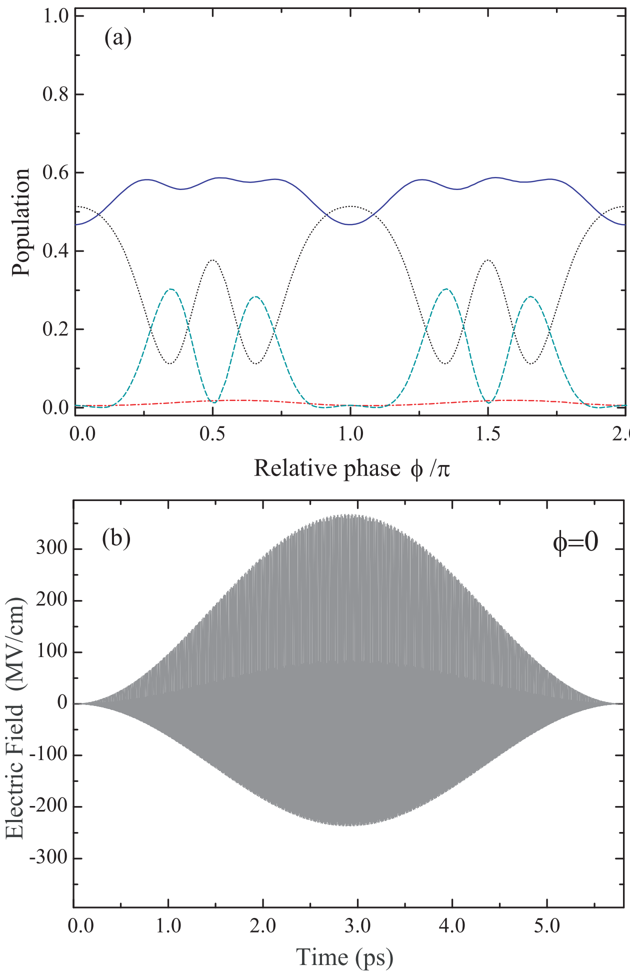

FIG. 3. (Color online) (a) The population distributions versus the relative phase ϕ. The solid, dot, dashed, and dot-dashed curves represent the states $|4,1\rangle$, $|0,0\rangle$, $|4,0\rangle$, and $|0,1\rangle$, respectively. (b) The total electric field with $\phi = 0$. The laser parameters are chosen to be $E_1 = 141.93$ MV/cm, $E_2 = 228.02$ MV/cm, $\tau_1 = \tau_2 = 5.805$ ps, $t_{01} = t_{02} = 0$ ps.

in the positive direction, as shown in Figs. 1(c) and 1(d). In Fig. 1(a) the population distributions are the same at $\phi = 0$ and $\phi = \pi$, which indicates that the asymmetry in direction has no effect on the population distributions. The shape of the total electric field varies from the largest asymmetry to a symmetry with a period of π, so there is a clear period of π in the population curves, which is similar to the processes of ionization and dissociation controlled by two harmonic pulses [20,23]. Besides the states $|4,1\rangle$ and $|0,0\rangle$, some population can be found in states $|4,0\rangle$ and $|0,1\rangle$. The population $P_{4,0}$ is derived from the multiphoton transitions according to Eqs. (8) and (9). A small amount of population is transferred to state $|0,1\rangle$ through two Λ transitions:

$$|0,0\rangle \xrightarrow{\omega} |1,1\rangle \xrightarrow{\omega} \left\{\begin{matrix}|2,0\rangle\\|2,2\rangle\end{matrix}\right\} \xrightarrow{2\omega} |0,1\rangle, \tag{12}$$

$$|0,0\rangle \xrightarrow{2\omega} |2,1\rangle \xrightarrow{\omega} \left\{\begin{matrix}|1,0\rangle\\|1,2\rangle\end{matrix}\right\} \xrightarrow{\omega} |0,1\rangle. \tag{13}$$

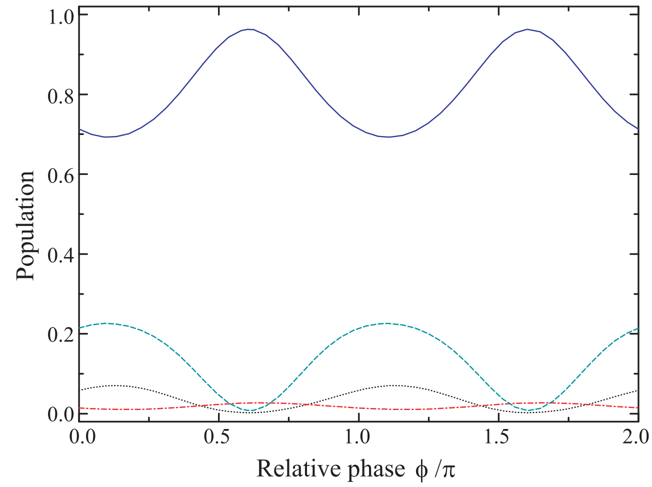

FIG. 4. (Color online) The population distributions versus the relative phase ϕ. The solid, dot, dashed, and dot-dashed curves represent the states $|4,1\rangle$, $|0,0\rangle$, $|4,0\rangle$, and $|0,1\rangle$, respectively. The laser parameters are chosen to be $E_1 = 159.90$ MV/cm, $E_2 = 173.79$ MV/cm, $\tau_1 = \tau_2 = 5.805$ ps, $t_{01} = 480\pi/\omega$ ps, $t_{02} = 0$ ps.

As the durations of two-color pulses are decreased from 8.708 ps to 7.257 and 5.805 ps, the optimal pulse amplitudes have to be increased to maintain a high population (nearly 100%) in the target state $|4,1\rangle$, as shown in Fig. 2. The maximal populations reach 98.3% and 96.8%, and the minimal populations are 14.6% and 0 in Figs. 2(a) and 2(b). We can see that curves of populations also oscillate with a period of π. In Fig. 2(c) the amplitudes of the total electric field in positive and negative directions are 286 and 145 MV/cm, and the size of the asymmetry ΔE is 141 MV/cm. For Figs. 1(c) and 2(d) the sizes of the asymmetry are 98 and 172 MV/cm, respectively. It can been seen from Figs. 1 and 2 that the size of the asymmetry is increased with the increase of optimal pulse amplitudes, and a larger size of the asymmetry can lead to a larger oscillation amplitude of the population curves. The size of the electric field asymmetry varies with the ratio of two pulse amplitudes.

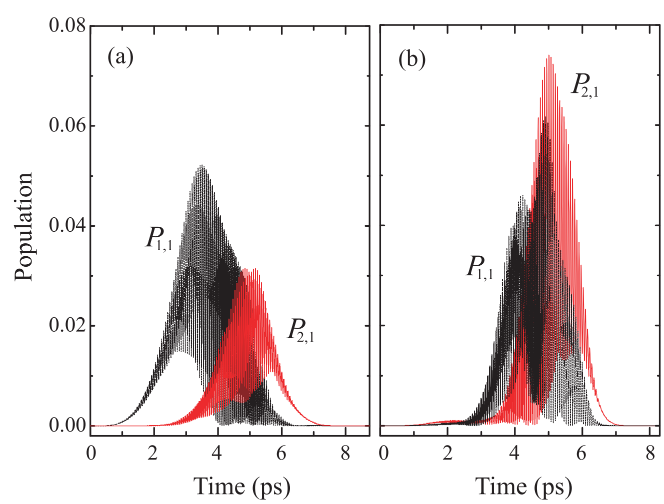

FIG. 5. (Color online) Time-dependent populations in the intermediate states $|1,1\rangle$ and $|2,1\rangle$. (a) The populations with $\phi = 0$ for Fig. 1(a). (b) The populations with $\phi = 0.60\pi$ for Fig. 4.

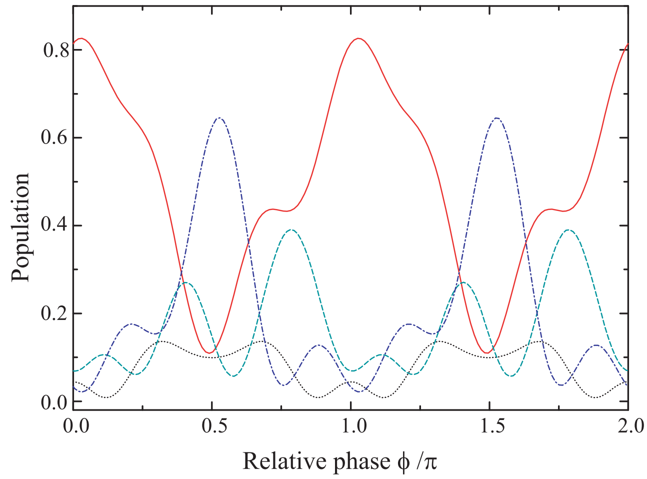

FIG. 6. (Color online) The population distributions versus the relative phase ϕ for a Λ system. The solid, dot, dashed, and dot-dashed curves represent the states $|0,1\rangle$, $|0,0\rangle$, $|4,0\rangle$, and $|4,1\rangle$, respectively. The laser parameters are chosen to be $E_1 = 228.29$ MV/cm, $E_2 = 239.37$ MV/cm, $\tau_1 = \tau_2 = 1.693$ ps, $t_{01} = t_{02} = 0$ ps.

In Fig. 3 the pulse durations and the sum of two amplitudes $E_1 + E_2$ are the same as those in Fig. 2(d), and the ratio of two amplitudes is varied. The oscillation amplitudes of the population curves for $|0,0\rangle$ and $|4,0\rangle$ in Fig. 3(a) are smaller than those in Fig. 2(b), and the oscillation of the population curves for the target state $|4,1\rangle$ is nearly wiped out. In Fig. 3(b) the size of the electric field asymmetry is 127 MV/cm, which is smaller than that in Fig. 2(d). This indicates that the oscillation amplitudes of the population curves depend on the size of the electric field asymmetry.

Usually, the ladder system is achieved by two partly overlapping pulses [13,14]. We have calculated the population transfer from $|0,0\rangle$ to $|4,1\rangle$, controlled by two partly overlapping pulses; the results are shown in Fig. 4. Because the delay time between the two pulses determines the relative phase, it should satisfy the condition $\Delta t = |t_{01} - t_{02}| = n\pi/\omega$, where n is the integer. In Fig. 4 the fundamental and second-harmonic pulses start at $480\pi/\omega$ and 0 ps, respectively. The maximum population values for the state $|4,1\rangle$ are at 0.6 and 1.60π, which are different from the values of relative phases in Fig. 1(a). We can see from Eqs. (10) and (11) that population is transferred to the state $|4,1\rangle$ via six intermediate states. Figure 5 shows the time-dependent populations for the intermediate states $|1,1\rangle$ and $|2,1\rangle$, which correspond to the (2+1) and (1+2) pathways, respectively. The parameters of the pulses in Fig. 5(a) are the same as those in Fig. 1(c). With these parameters, the peak value for population $P_{1,1}$ is larger than that for $P_{2,1}$ in Fig. 5(a),

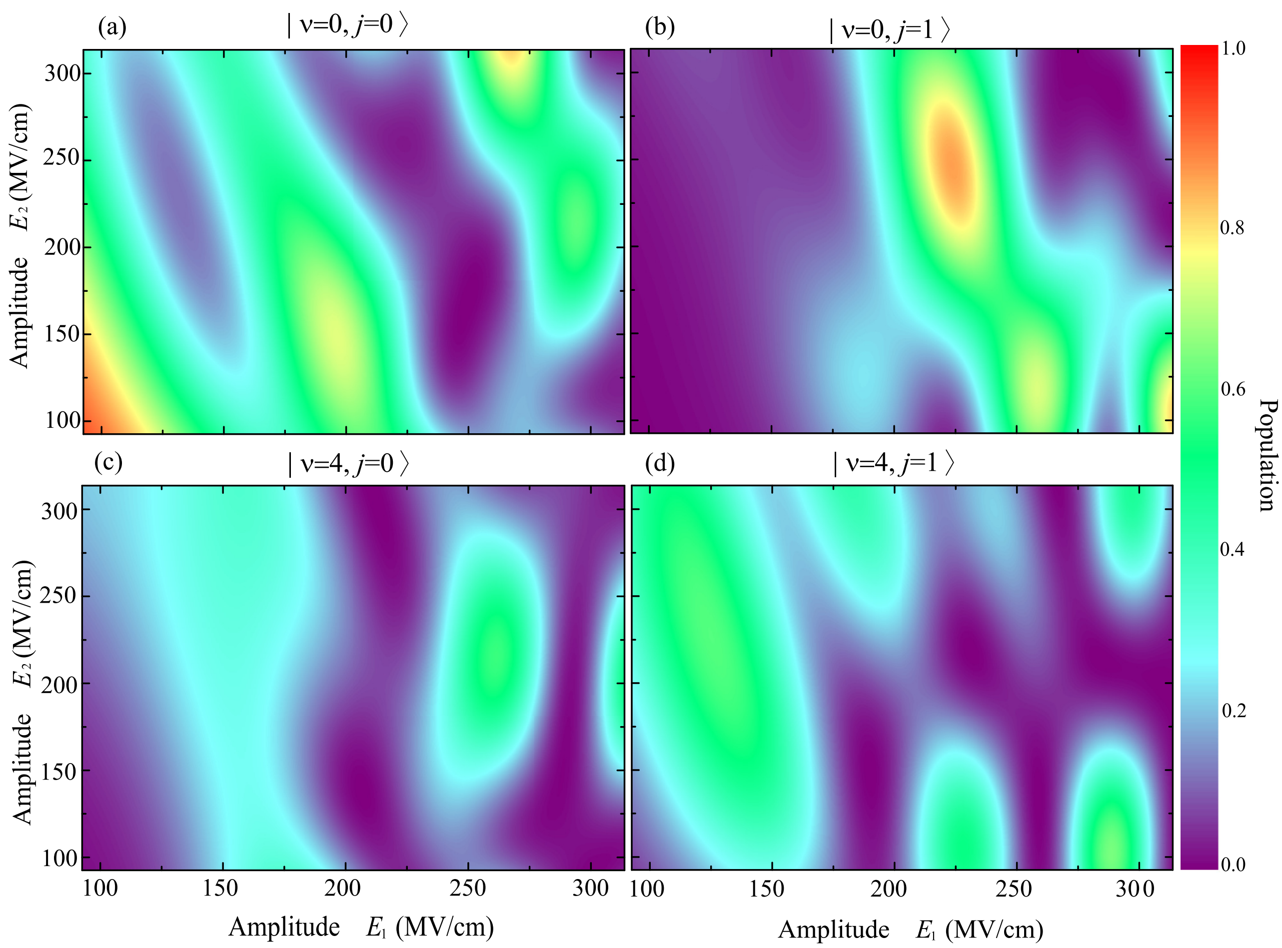

FIG. 7. (Color online) The population distributions as a function of amplitudes E_1 and E_2. (a) The population for the state $|0,0\rangle$. (b) The population for the state $|0,1\rangle$. (c) The population for the state $|4,0\rangle$. (d) The population for the state $|4,1\rangle$. The durations and start times of the two pulses are the same as those in Fig. 6.

and the maximum population values are at $\phi = 0$ and π in Fig. 1(a). In Fig. 5(b) the transitions do not take place before the fundamental pulse is turned on ($t_{01} = 2.158$ ps). When $t > 2.158$ ps, some population is transferred to the states $|1,1\rangle$ and $|2,1\rangle$, and the peak value for population $P_{2,1}$ is larger than that for $P_{1,1}$. In Figs. 5(a) and 5(b) the ratio of two peak values for $P_{1,1}$ and $P_{2,1}$ is different, which indicates the ratio of transitions through (1+2) and (2+1) pathways is different. The variation of the transition ratio causes the difference in the relative phases corresponding to the maximal population.

We now consider a Λ process in which the initial and target states are $|0,0\rangle$ and $|0,1\rangle$. The population transfer is achieved according to Eqs. (12) and (13). The fundamental frequency is still chosen as 3708.68 cm^{-1}; the other optimal parameters of the two pulses are shown in Fig. 6. Compared with the ladder system, the pulse durations for the Λ system are decreased, and the amplitudes are increased. It can be seen that the Λ transition is accompanied by the ladder and multiphoton transitions. Because some population is transferred to the states $|4,0\rangle$ and $|4,1\rangle$, the maximum value of population $P_{0,1}$ is only 82.6% at $\phi = 0.03\pi$ and 1.03π. The variation of population $P_{0,1}$ with the relative phase has a period of π, which is similar to those in the above cases.

We can see from the above cases that the transition probabilities through the ladder Λ and multiphoton transitions depend on the pulse amplitudes. Figure 7 shows the population distributions versus the pulse amplitudes E_1 and E_2. In Fig. 7(a) most of the population stays in the initial state $|0,0\rangle$ as $E_1 < 125$ and $E_2 < 150$ MV/cm. For the Λ transition, the final population of the target state $|0,1\rangle$ is small in Fig. 7(b), as $E_1 < 150$ MV/cm. The maximal population can be found in the region of $E_1 = 220$ and $E_2 = 240$ MV/cm. Compared with Fig. 7(b), the multiphoton and ladder transitions can take place with lower pulse amplitudes in Figs. 7(c) and 7(d). It can be seen from the population distributions of three target states that the region of $P > 0.4$ in Fig. 7(d) is larger than those in Figs. 7(b) and 7(c). This means that the ladder transition occurs more easily by controlling the two pulse amplitudes.

IV. CONCLUSION

In this article, we have studied the rovibrational dynamics of population transfer controlled by two-color laser pulses with fundamental and second-harmonic frequencies. The two coherent pulses can drive the ladder Λ and multiphoton transitions at the same time. The population distributions through these three transitions depend on the relative phase. The asymmetry in direction has no effect on the population distributions, and the size of electric field asymmetry determines the population variation with the relative phase. By choosing suitable pulse parameters, about 100% of the population can be transferred to state $|4,1\rangle$ through the ladder transition. The variation of the transition ratio through (1+2) and (2+1) pathways affects the relative phase corresponding to the maximal population. The transition probabilities for states $|4,1\rangle$, $|0,1\rangle$, and $|4,0\rangle$ depend on the two pulse amplitudes. Compared with the Λ transition, the ladder transition takes place more easily by controlling the amplitudes of the two-color pulses.

ACKNOWLEDGMENTS

This work is supported by the National Natural Science Foundation of China under Grants No. 11347012 and No. 21473018.

[1] H. T. K. Bergmann and B. W. Shore, Rev. Mod. Phys. **70**, 1003 (1998).
[2] M. V. Korolkov, G. K. Paramonov, and B. Schmidt, J. Chem. Phys. **105**, 1862 (1996).
[3] N. V. Vitanov and B. W. Shore, Phys. Rev. A **73**, 053402 (2006).
[4] E. A. Shapiro, A. Pe'er, J. Ye, and M. Shapiro, Phys. Rev. Lett. **101**, 023601 (2008).
[5] S. Chelkowski, A. D. Bandrauk, and P. B. Corkum, Phys. Rev. Lett. **65**, 2355 (1990).
[6] B. M. Garraway and K. A. Suominen, Phys. Rev. Lett. **80**, 932 (1998).
[7] Y. N. Demkov and V. N. Ostrovsky, Phys. Rev. A **61**, 032705 (2000).
[8] S. Shi, A. Woody, and H. Rabitz, J. Chem. Phys. **88**, 6870 (1988).
[9] T. Hornung, M. Motzkus, and R. de Vivie-Riedle, Phys. Rev. A **65**, 021403(R) (2002).
[10] I. V. Andrianov and G. K. Paramonov, Phys. Rev. A **59**, 2134 (1999).
[11] S. Schiemann, A. Kuhn, S. Steuerwald, and K. Bergmann, Phys. Rev. Lett. **71**, 3637 (1993).
[12] C.-C. Shu, J. Yu, K.-J. Yuan, W.-H. Hu, J. Yang, and S.-L. Cong, Phys. Rev. A **79**, 023418 (2009).
[13] N. N. Bezuglov, R. Garcia-Fernandez, A. Ekers, K. Miculis, L. P. Yatsenko, and K. Bergmann, Phys. Rev. A **78**, 053804 (2008).
[14] R. Bhattacharya, S. Chatterjee, and S. S. Bhattacharyya, Phys. Rev. A **80**, 063423 (2009).
[15] I. Vrábel and W. Jakubetz, J. Chem. Phys. **118**, 7366 (2003).
[16] Y.-Y. Niu, R. Wang, and M.-H. Qiu, Phys. Rev. A **84**, 023406 (2011).
[17] E. Charron, A. Giusti-Suzor, and F. H. Mies, Phys. Rev. Lett. **71**, 692 (1993).
[18] A. D. Bandrauk and S. Chelkowski, Phys. Rev. Lett. **84**, 3562 (2000).
[19] S. Chelkowski, M. Zamojski, and A. D. Bandrauk, Phys. Rev. A **63**, 023409 (2001).
[20] H. Ohmura, T. Nakanaga, and M. Tachiya, Phys. Rev. Lett. **92**, 113002 (2004).
[21] S.-M. Wang, K.-J. Yuan, Y.-Y. Niu, Y.-C. Han, and S.-L. Cong, Phys. Rev. A **74**, 043406 (2006).
[22] M. Spanner, S. Patchkovskii, E. Frumker, and P. Corkum, Phys. Rev. Lett. **109**, 113001 (2012).
[23] B. Sheehy, B. Walker, and L. F. DiMauro, Phys. Rev. Lett. **74**, 4799 (1995).
[24] C. C. Marston and G. G. Balint-Kurti, J. Chem. Phys. **91**, 3571 (1989).
[25] M. D. Feit, J. A. Fleck Jr., and A. Steiger, J. Comput. Phys. **47**, 412 (1982).
[26] R. Wang, J.-L. Xiu, and Y.-Y. Niu, Acta Phys. Sin. **62**, 093301 (2013).